

# Parametric study of a radio-frequency glow discharge using a continuum model

Sang-Kyu Park<sup>a)</sup> and Demetre J. Economou<sup>b)</sup>

Department of Chemical Engineering, University of Houston, Houston, Texas 77204-4792

(Received 5 January 1990; accepted for publication 25 July 1990)

An efficient numerical algorithm was developed to solve the continuity equations describing charged particle transport and potential distribution in a low-pressure glow discharge in an argonlike gas. A parametric investigation of the effect of gas pressure and electrode spacing on the discharge properties was conducted.

Plasma etching and deposition of thin films, using low-pressure radio-frequency (rf) gas discharges, is of paramount importance in the modern microelectronics industry. Despite the extensive use of gas plasmas, the intricate nature of the glow discharge is poorly understood. This is in part due to the complex interaction between charged particle kinetics and potential distribution in the discharge. Continuum models of glow discharges<sup>1-6</sup> appear to be useful in an effort to better understand the discharge physics. Furthermore, coupling of the glow-discharge models with the rather well-developed neutral transport and reaction models<sup>7</sup> could result in powerful tools for the analysis and design of plasma reactors. The models must be tested with experimental observations<sup>8</sup> to upgrade the assumptions and to extend the range of validity.

Continuum models for the glow discharges of interest consist of a set of partial differential equations describing the mass, momentum, and energy balance for electrons and ions (positive and negative), coupled to the Poisson equation for the potential distribution. Because of the severe numerical complexity of the problem, simplifying assumptions are introduced, limiting the parameter range over which the models are applicable. Despite the simplifying assumptions, the model equations are still very difficult to solve because the system is stiff in both space and time. The excessive computational time requirements limit the utility of the models and hamper the extension of the models to more realistic systems. Hence, the search for efficient numerical techniques to solve the model equations continues.

In the present work, the model equations were solved by the method of lines using orthogonal collocation on finite elements for the spatial discretization. The efficiency of the numerical algorithm allowed for a parametric investigation of an argonlike glow discharge to be conducted using a reasonable amount of computer time. The effect of gas pressure and electrode spacing on the discharge properties was studied.

The model equations used in the present work were the same as in the work of Graves.<sup>2</sup> However, a larger peak-to-peak applied rf voltage was used, the whole interelectrode gap was modeled (no push-pull arrangement), and the temperature dependence of the reaction rate in the

charged species continuity equations was retained (instead of using a constant mean temperature). The model equations are written as

$$\frac{\partial n_e}{\partial t} + \nabla \cdot \mathbf{J}_e = R_i, \quad (1)$$

$$\frac{\partial n_+}{\partial t} + \nabla \cdot \mathbf{J}_+ = R_i, \quad (2)$$

$$\mathbf{J}_e = -D_e \nabla n_e + n_e \mu_e \nabla V, \quad (3)$$

$$\mathbf{J}_+ = -D_+ \nabla n_+ - n_+ \mu_+ \nabla V, \quad (4)$$

$$\frac{\partial}{\partial t} \left( \frac{3}{2} n_e k T_e \right) + \nabla \cdot \mathbf{q}_e - e \mathbf{J}_e \cdot \nabla V + \sum_j H_j R_j = 0, \quad (5)$$

$$\mathbf{q}_e = -K_e \nabla T_e + \frac{5}{2} k T_e \mathbf{J}_e, \quad (6)$$

$$\nabla^2 V = - (e/\epsilon_0) (n_+ - n_e), \quad (7)$$

$$R_i = k_{i0} n_e N \exp[ - (E_i/kT_e) ], \quad (8)$$

$$R_{ex} = k_{ex0} n_e N \exp[ - (E_{ex}/kT_e) ]. \quad (9)$$

Equations (1) and (2) are the electron and ion continuity equations, respectively, Eqs. (3) and (4) are in essence the momentum balance for the electrons and ions, respectively, and Eq. (5) is the electron energy balance, with the total electron energy flux given by Eq. (6). Equation (7) is the Poisson equation for the potential distribution in the gap, and Eqs. (8) and (9) provide expressions for the ionization and excitation rate, respectively. In the above equations,  $n_e$  and  $n_+$  are the electron and ion density, respectively,  $\mathbf{J}_e$  and  $\mathbf{J}_+$  are the electron and ion flux, respectively,  $T_e$  is the electron temperature, and  $\mathbf{q}_e$  is the electron energy flux. Moreover,  $N$  is the neutral gas density,  $V$  is the potential,  $k_{i0}$  and  $k_{ex0}$  are the preexponential factors in Eqs. (8) and (9), respectively,  $E_i$  and  $E_{ex}$  are the activation energy for ionization and excitation, respectively,  $D_e$  is the electron diffusivity,  $\mu_e$  is the electron mobility,  $D_+$  is the ion diffusivity, and  $\mu_+$  is the ion mobility.  $H_i$  and  $H_{ex}$  are the electron energy loss per ionizing and

<sup>a)</sup>Current address: Advanced Products Research and Development Laboratory, Motorola Inc., 3501 Ed Bluestein Boulevard, Austin, TX 78721.

<sup>b)</sup>Author to whom correspondence should be addressed.

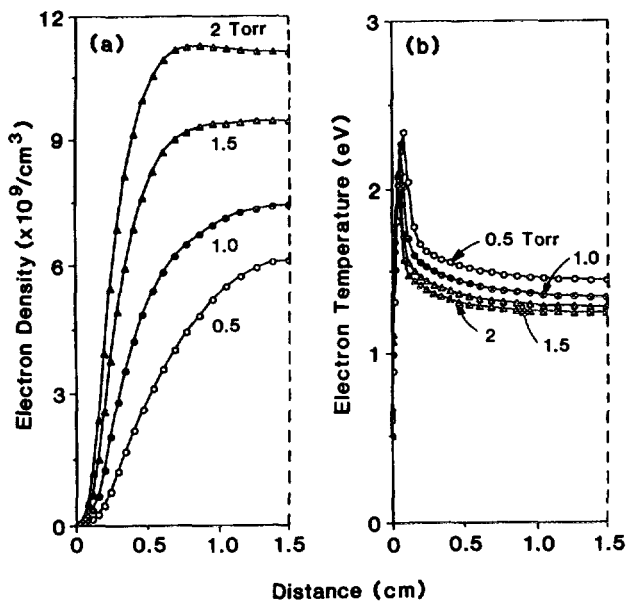


FIG. 1. Time-averaged electron density (a) and electron temperature (b) in the gap for different pressures.

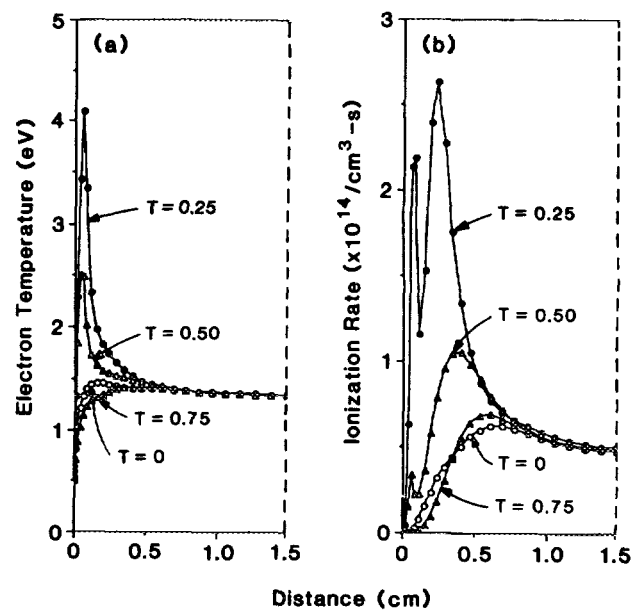


FIG. 2. Spatial and temporal variation of electron temperature (a) and ionization rate (b) for a pressure of 1 Torr.

exciting collision, respectively, and  $\epsilon_0$  is the permittivity of the free space. The parameter values used were the same as in Ref. 9.

Boundary conditions on electron flux and ion flux were the same as in Ref. 2. The left electrode was driven with a voltage of the form  $V = -V_{rf} \sin(2\pi ft)$ , and the right electrode was assumed to be grounded ( $V = 0$ ). The peak rf voltage was 25 V (50 V peak to peak), and the excitation frequency  $f$  was 10 MHz. The boundary condition on the electron temperature is difficult to specify.<sup>2</sup> A constant temperature of 0.5 eV was used for both electrodes. The parameters varied in this study were pressure (values examined are 0.5, 1.0, 1.5, and 2 Torr), and interelectrode spacing (values examined are 1.5, 3.0, 4.5, and 6.0 cm).

The coupled system of parabolic and elliptic partial differential equations was solved by the method of lines.<sup>10</sup> The equations were discretized in the spatial direction using orthogonal collocation on finite elements,<sup>11</sup> with  $B$ -spline (cubic polynomial) basis functions.<sup>12</sup> The resulting system of differential-algebraic equations was solved by an implicit variable-order, variable-time step, backward-difference formula.<sup>13</sup> 50 finite elements were used, with smaller element size near the electrodes, where steep gradients are expected. The resulting system of 408 equations was solved in double precision on an NEC SX-2 supercomputer. For a pressure of 1 Torr and a spacing of 3 cm, the execution time was 20 central processing unit (CPU) mins. Details on the numerical algorithm along with the effect of frequency and peak voltage are presented elsewhere.<sup>9</sup>

Figure 1(a) shows the time-averaged electron density distribution in the gap, for a spacing 3 cm, and for different pressures (or neutral number densities  $N$ , for constant  $T$ ). The ion density profiles were identical except for the sheath regions near the electrodes, where the ion density exceeded

the electron density. Figure 1(b) shows the corresponding electron temperature distributions. Owing to symmetry, only half of the interelectrode space is shown. As pressure increases, the electron density profile becomes flatter in the bulk plasma, and the sheath thickness decreases. The electron temperature peaks near the plasma-sheath boundary as the oscillating sheaths impart energy to the electrons. The electron temperature decreases with increasing pressure since the mean free path of the electrons decreases. Hence, the electrons pick up less energy from the electric field in the time between collisions. The decrease in the mean free path with pressure is also responsible for the peak in electron temperature appearing nearer the electrode as the pressure increases. However, the electron temperature is not a strong function of pressure in the range of the parameter values examined. In the relatively high-pressure, high-frequency regime, for which secondary electrons do not penetrate the bulk, the glow may resemble the positive column. The electron temperature in the positive column is often expressed as a function of the product  $p\Lambda$ ,<sup>14</sup> where  $\Lambda$  is the electron diffusion length (equal to  $L/\pi$  for infinite parallel plates). For the range of  $p\Lambda$  values covered in Fig. 1 (0.48–1.91 Torr cm), the electron temperature in argon plasmas has been found to be a weak function of  $p\Lambda$ .<sup>14</sup> The power density was found to increase from 1.86 mW/cm<sup>2</sup> for 0.5 Torr to 3.34 mW/cm<sup>2</sup> for 2 Torr. For the basic conditions (3 cm spacing and 1 Torr), the current waveform was found to lag the voltage waveform by about 80°.

The spatial distribution of electron temperature and ionization rate at different fractions of the rf cycle are shown in Fig. 2. Time  $T = 0$  corresponds to the negative zero crossing of the potential waveform (thus  $T = 0 - 0.5$  corresponds to the part of the cycle for which the left electrode is the cathode). Only the left half of the interelectrode space is shown. The behavior on the right half

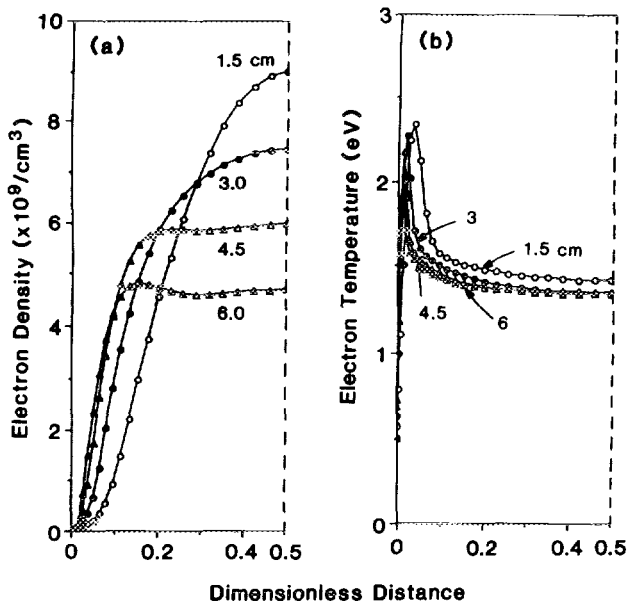


FIG. 3. Time-averaged electron density (a) and electron temperature (b) in the gap for different spacings. Pressure was 1 Torr.

can be obtained by flipping the plot horizontally, and adding 0.5 to the time. One observes that the electron temperature and ionization rate are modulated only near the electrodes. Sharp electron temperature gradients are observed in the sheath region, especially when the electrode potential has attained its peak negative value (for  $T = 0.25$ ). Then, electrons which had diffused near the electrode earlier in the cycle, are "pushed" towards the bulk plasma by the expanding sheath front. The ionization is also concentrated near the plasma-sheath boundary where the product of electron density and ionization rate constant is high. A double peak in the ionization rate is observed especially when the electrode potential has its maximum negative value ( $T = 0.25$ ). The first peak (nearer the electrode) is associated with the peak in electron temperature [see Fig. 1(a)]. The electron density nearer the electrode is low, and this is the reason the first peak is lower than the second peak. The second peak forms further away from the electrode where the electron density is high, and yet the electron temperature has not decayed to its lowest value.

The effect of interelectrode spacing on the time-averaged electron density and electron temperature is shown in Fig. 3, where a dimensionless axial coordinate has been used to consolidate the results. The pressure was set at 1 Torr. The electron density decreases with increasing spacing, since the power density ( $\text{W}/\text{cm}^3$ ) decreases

with spacing at constant applied voltage (in this case 50 V peak to peak). In addition, the electron density profile becomes flatter in the bulk plasma as the spacing increases. Further, the fraction of the gap length occupied by the sheath decreases with increasing spacing. The electron temperature decreases with increasing spacing. However, the dependence of  $T_e$  on spacing is rather weak for the parameter values used. If the bulk electron temperature were a unique function of  $p\Lambda$  (as in the positive column), values of  $T_e$  in the bulk plasma obtained from Figs. 1(b) and 3(b) should have been identical for all combinations of  $p$  and  $\Lambda$  resulting in the same value of  $p\Lambda$ . One concludes that the bulk plasma in the present case cannot be considered as strictly equivalent to a positive column.

In summary, an efficient numerical algorithm, based on the method of lines and collocation on finite elements, has been developed to solve the continuity equations describing charged particle transport and potential distribution in an argonlike glow discharge. Parametric studies of the effect of pressure and electrode spacing on the electron density and temperature distributions have been presented. The ultimate goal is to couple the glow-discharge models with neutral species transport and reaction models to predict etching (or deposition) rate, uniformity, and anisotropy.

We are grateful to the National Science Foundation (CBT-8708908), to Texas Instruments and to the Welch Foundation for financial support. Thanks are due to the Houston Advanced Research Center (HARC) for an NEC SX-2 supercomputer-time grant. S.-K. Park was partially supported by the Ministry of Education, Republic of Korea.

- <sup>1</sup>D. B. Graves and K. F. Jensen, *IEEE Trans. Plasma Sci.* **PS-14**, 78 (1986).
- <sup>2</sup>D. B. Graves, *J. Appl. Phys.* **62**, 88 (1987).
- <sup>3</sup>A. D. Richards, B. E. Thompson, and H. H. Sawin, *Appl. Phys. Lett.* **50**, 492 (1987).
- <sup>4</sup>E. Gogolides, J.-P. Nicolai, and H. H. Sawin, *J. Vac. Sci. Technol. A* **7**, 1001 (1989).
- <sup>5</sup>M. S. Barnes, T. J. Cotler, and M. E. Elta, *J. Comput. Phys.* **77**, 53 (1988).
- <sup>6</sup>J.-P. Boeuf, *Phys. Rev. A* **36**, 2782 (1987).
- <sup>7</sup>S.-K. Park and D. J. Economou, *J. Electrochem. Soc.* **137**, 2624 (1990).
- <sup>8</sup>R. A. Gottscho and M. L. Mandich, *J. Vac. Sci. Technol. A* **3**, 617 (1985).
- <sup>9</sup>S.-K. Park and D. J. Economou, *J. Appl. Phys.* **68**, 3904 (1990).
- <sup>10</sup>L. Lapidus and W. E. Schiesser, *Numerical Methods for Differential Systems* (Academic, New York, 1976).
- <sup>11</sup>B. A. Finlayson, *Numerical Methods in Chemical Engineering* (McGraw-Hill, New York, 1980).
- <sup>12</sup>C. deBoor, *A Practical Guide to Splines* (Springer, New York, 1978).
- <sup>13</sup>A. C. Hindmarsh, in *Scientific Computing*, edited by R. Stepleman (IMACS, North-Holland, Amsterdam, 1983), p. 55.
- <sup>14</sup>A. Cantin and R. R. Cagne, *Appl. Phys. Lett.* **30**, 316 (1977).